

## EFFECT OF MO CONTENT IN MO(X)/ $\gamma$ -AL<sub>2</sub>O<sub>3</sub> CATALYSTS OVER THE CONVERSION OF 2-METHOXYPHENOL AS LIGNIN-DERIVATES COMPONENTS

K. LEIVA<sup>a</sup>, C. SEPÚLVEDA<sup>a</sup>, R. GARCÍA<sup>a</sup>, J. L. G. FIERRO<sup>b</sup>, P. REYES<sup>a</sup>, I. T. GHAMPSON<sup>c</sup>, P. BAEZA<sup>d</sup>, M. VILLARROEL<sup>e</sup>, N. ESCALONA<sup>a\*</sup>

<sup>a</sup> Universidad de Concepción, Facultad de Ciencias Químicas, Casilla 160C, Concepción, Chile.

<sup>b</sup> Instituto de Catálisis y Petroquímica, CSIC, Cantoblanco, 28049 Madrid, Spain.

<sup>c</sup> Unidad de Desarrollo Tecnológico, Universidad de Concepción, Casilla 4051, Concepción, Chile

<sup>d</sup> Pontificia Universidad Católica de Valparaíso, Facultad de Ciencias, Instituto de Química, Casilla 4059, Valparaíso, Chile

<sup>e</sup> Universidad Católica Silva Henríquez, Facultad de Educación, General Jofré 462, Santiago, Chile

(Received: May 10, 2013 - Accepted: July 8, 2013)

### ABSTRACT

The effect of Mo loading (10, 12, 15, 17 and 20 wt.%) on the physicochemical properties and reactivities of Mo(x)/ $\gamma$ -Al<sub>2</sub>O<sub>3</sub> sulfide catalysts for the conversion of 2-methoxyphenol at 573 K and 5 MPa of hydrogen pressure were studied. The catalysts were characterized by specific area ( $S_{\text{BET}}$ ), electrophoretic migration (EM), X-ray photoelectron spectroscopy (XPS) and surface acidity techniques. The highest conversion observed for the catalyst with a Mo loading of 15 wt.% was attributed to an increase in the number of active sites due to highly dispersed Mo species. At higher Mo loadings, the formation of Mo aggregates led to lower guaiacol conversion. The differences in the phenol/catechol ratio were explained by the acid strengths of the sulfided catalysts.

**Keywords:** hydrodeoxygenation, 2-methoxyphenol, MoS<sub>2</sub>, acid strength.

### 1. INTRODUCTION

The increase in world energy demand during the 21<sup>st</sup> century and the limited oil reserves, in part, have driven the industry to look for new and alternative energy sources. In this regard, biomass has generated considerable interests because of its renewability and its inertness with respect to CO<sub>2</sub> emissions. The fast pyrolysis of woody biomass leads to the formation of char, gases and liquid products known as bio-oil (liquor or pyrolygneous acid) [1]. However, due to its instability and undesirable properties, it is impossible to directly use the generated bio-oil as an alternative fuel to conventional petroleum fuels. Consequently, studies focusing on upgrading of bio-oil to fungible fuels using hydrodeoxygenation (HDO) catalysts have received renewed interests [2, 3]. A great number of these studies used model compounds to stimulate the catalytic HDO process: 2-methoxyphenol (guaiacol), a highly representative organic-phase compound of bio-oil, has commonly been used because it possesses two different oxygenated functional groups (phenolic and methoxy groups) and also because of its refractory character to complete deoxygenation [4].

In recent years, the catalytic behaviors of metals [5], nitrides [6] and sulfides [7, 8, 9, 10, 11, 12, 13] for the conversion of guaiacol have been studied. Bui *et al.* [13] studied the effect of support of MoS<sub>2</sub> catalysts on the activity and selectivity of the HDO of guaiacol. The authors found that the acidity of the supports greatly influences guaiacol transformation routes and possible catalyst deactivation (through coke deposition on the active sites). However, it is important to point out that the acidity of the support does not have exclusive control on activity and selectivity: morphological changes in MoS<sub>2</sub>, induced by differences in dispersion, as suggested Hensen *et al.* [14] in the hydrotreating of thiophene, dibenzothiophene and toluene, can also influence activity and selectivity. The authors reported that increase in the average layer stacking degree of supported MoS<sub>2</sub> catalysts favored the hydrogenation pathway due to the adsorption on the edges of lamellar structures. In addition, Yang *et al.* [15] demonstrated that low stacking of MoS<sub>2</sub> slabs favored hydrogenolysis over hydrogenation during the conversion of phenols over bulk MoS<sub>2</sub>. For supported catalysts these results may also depend on the MoS<sub>2</sub> content. However, this is a largely unexplored area of HDO catalysis.

The main objective of this work was to study the changes in the activity and selectivity in the HDO of guaiacol, influenced by differences in the Mo loadings of  $\gamma$ -Al<sub>2</sub>O<sub>3</sub>-supported MoS<sub>2</sub> catalysts.

### 2. EXPERIMENTAL

#### 2.1 Catalyst preparation

Molybdenum-based catalysts were prepared by the wet impregnation method using excess solvent, (NH<sub>4</sub>)<sub>6</sub>Mo<sub>7</sub>O<sub>24</sub>·4H<sub>2</sub>O as Mo precursor and

$\gamma$ -Al<sub>2</sub>O<sub>3</sub> (Gilder T-126) as support. The Mo loadings used for the catalysts preparation were 10, 12, 15, 17 and 20 wt. %. The impregnated catalysts were dried at 393 K for 8 h and then calcined at 823 K for 4 h.

#### 2.2 Characterization of the Catalysts

The specific area ( $S_{\text{BET}}$ ) and pore volume ( $V_p$ ) of the catalysts were determined from nitrogen isotherms at 77 K using a Micromeritics ASAP 2010 equipment.

The surface acidity was performed by potentiometric titration [16], adding 0.05 mL of a solution of butylamine in dissolution of 150 mg of sample in acetonitrile (0.1 mol / L<sup>-1</sup>) in constant agitation with a magnetic stirrer. The solution was agitated for 3h and then continuing the addition of 0.05 mL of butylamine in acetonitrile every 2 minutes until the potentiometric curve tends to a constant value of the potential. The glass electrode of Ag / AgCl was used and a pH-meter Mettler Toledo MP 220.

Electrophoretic migration (EM) measurement were performed using a Zeta-Meter Inc. 3.0 apparatus using 30 mg of sample suspended in 300 mL of KCl (10<sup>-3</sup> molL<sup>-1</sup>). KOH or HCl solutions (0.1 mol L<sup>-1</sup>) were used for pH adjustment. The zero point charge (ZPC) for all catalysts was obtained from the plot of pH vs. zeta potential, corresponding to the pH value where the curve intersects the abscissa.

X-ray photoelectron spectra (XPS) of sulfide catalysts were obtained on an Microtech Multilab 3000 spectrometer, equipped with a hemispherical electron analyzer and MgK $\alpha$  (1253.6 eV) photon source. Prior to the measurements, the catalysts samples were pre-sulfided *ex-situ* under a flow of 10% H<sub>2</sub>S/H<sub>2</sub> mixture at 623 K for 4 h. The binding energies (BE) at 74.4 eV were referenced to the Al 2p level of the alumina support.

#### 2.3 Catalytic tests

HDO of guaiacol was carried out in an autoclave reactor operating in the batch mode at 573 K under pressure of 50 bar of H<sub>2</sub>. The liquid reactant mixture, 0.232 molL<sup>-1</sup> of guaiacol, 0.0125 mol L<sup>-1</sup> of CS<sub>2</sub>, 80 mL of decalin and 700  $\mu$ L of hexadecane (internal standard) were introduced to the reactor containing 250 mg of pre-sulfided catalyst (*ex-situ* at 623 K for 4 h under 10% H<sub>2</sub>S/H<sub>2</sub> flow). The system was closed, and to avoid any air contamination, N<sub>2</sub> was bubbled through the dispersion for 10 min. Still under N<sub>2</sub>, the reactor was heated up to the reaction temperature of 573 K under constant stirring. When the reaction temperature was reached, the H<sub>2</sub> pressure was introduced into the reactor up to 50 bar of H<sub>2</sub>. The pressure was kept constant during the course of the experiment by monitoring the high pressure manometer. Samples were taken periodically during the reaction, through a sample outlet with a temperature below 40 °C, ensuring that all samples are in liquid phase. The samples were analyzed on a Perkin Elmer CG (autosystem XL), with a

semicapilar column CPSIL-5CB. The specific rate for the total conversion of guaiacol was deduced from the plot of the initial slope of conversion as a function of time, and expressed in mol g<sup>-1</sup> s<sup>-1</sup>.

The selectivities (%) of phenol and catechol were determined at 10% conversion of guaiacol according to Eq. 1:

$$S_{(\%)} = \frac{X_i}{X_T} \cdot 100 \quad (\text{Eq. 1})$$

Where X<sub>i</sub> is the percentage of formation of phenol or catechol, and X<sub>T</sub> is the guaiacol conversion at 10%. The phenol/catechol ratio was then determined from the respective selectivities of each compound.

## RESULTS AND DISCUSSION

### 3.1 Characterization of Mo(x)/γ-Al<sub>2</sub>O<sub>3</sub> catalysts.

The specific area (S<sub>BET</sub>) and total pore volume (Vp) of calcined Mo(x)/γ-Al<sub>2</sub>O<sub>3</sub> catalysts are shown in Table 1. It can be seen that the S<sub>BET</sub> and Vp decrease gradually with the Mo content increases. This result suggests that Mo was well deposited inside the pores of the γ-Al<sub>2</sub>O<sub>3</sub> support, and that pore blockage was limited.

Figure 1 shows the effect of pH on the zeta potential (ZP) of the Mo(x)/γ-Al<sub>2</sub>O<sub>3</sub> catalysts. The ZPC initially decreased gradually with increasing Mo loading up to 15 wt.%. At higher Mo loading, the ZPC was nearly constant around a value of 6.8; this behavior is more clearly illustrated on the inset of Figure 1. The decrease in the ZPC indicates that the Mo species present a homogeneous distribution on the surface of alumina; the invariability of the ZPC for catalysts with Mo loadings higher than 15 wt.% indicates that the coverage of the free-surface of the support by Mo species was stalled because of their likely deposition in the form of multilayers. Similar behavior has been previously observed by Gil-Llambias *et al.* [17].

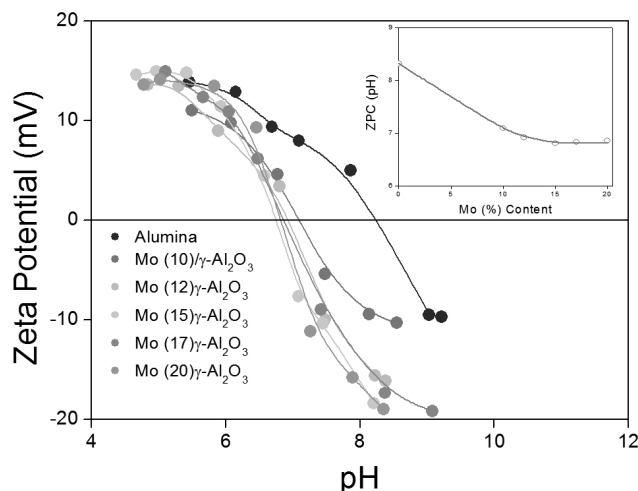


**Figure 1:** Effect of pH on the zeta potential of the alumina support and Mo(x)/γ-Al<sub>2</sub>O<sub>3</sub> catalysts. Inset: variation of the zero point charge (ZPC) of Mo(x)/γ-Al<sub>2</sub>O<sub>3</sub> catalysts with Mo loading.

**Table 1.** Mo content, specific surface area (S<sub>BET</sub>) and total pore volume (Vp) of oxidized samples.

Catalysts	Mo (%)	Vp (cm <sup>3</sup> g <sup>-1</sup> )	S <sub>BET</sub> (m <sup>2</sup> g <sup>-1</sup> )
γ-Al <sub>2</sub> O <sub>3</sub>	--	0.38	220
Mo(10)/γ-Al <sub>2</sub> O <sub>3</sub>	10	0.36	210
Mo(12)/γ-Al <sub>2</sub> O <sub>3</sub>	12	0.36	200
Mo(15)/γ-Al <sub>2</sub> O <sub>3</sub>	15	0.34	190
Mo(17)/γ-Al <sub>2</sub> O <sub>3</sub>	17	0.30	170
Mo(20)/γ-Al <sub>2</sub> O <sub>3</sub>	20	0.31	170

Figure 2 shows the acid strength of the calcined and sulfided Mo(x)/γ-Al<sub>2</sub>O<sub>3</sub> catalysts as functions of the Mo loading. For the calcined catalysts it is possible to observe that the acid strength increases with Mo loading up to 15 wt.%. According to the interpretation of the values of the initial electrode potential (E<sub>i</sub>) [16], the catalysts exhibited very strong acid sites. These strong acid sites can be attributed to Mo-OH terminal bonds from supported molybdenum oxide monomeric or polymeric species. Effectively, Topsøe and Topsøe [18] showed that a low Mo concentration, the active phase has a preferential interaction with the surface hydroxyl groups of alumina, and may form tetrahedrally coordinated Mo species, leading to Mo-OH terminal bonds.

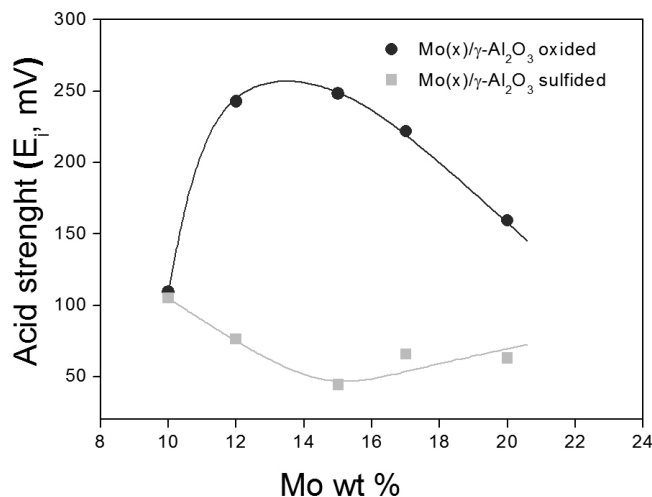


**Figure 2:** Effect of Mo loading on acid strength of oxidized and sulfided Mo(x)/γ-Al<sub>2</sub>O<sub>3</sub> catalysts.

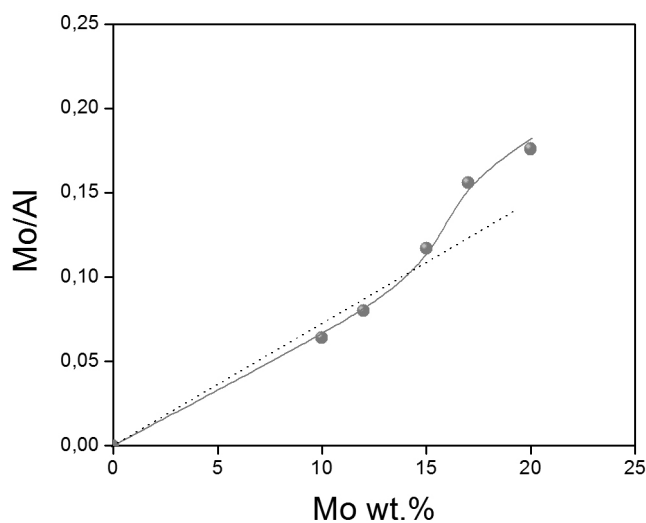
The decrease in acid strength at Mo loadings over 15 wt.% is attributed to growth in formation of three dimensional MoO<sub>3</sub> particles, [19], probably forming clusters (Mo-O-Mo species) which decreases Mo-OH groups, in agreement with the results from EM measurements. Moreover, Figure 2 shows that after sulfidation the acid strength of the catalysts decreased significantly. This trend can be attributed to the fact that the sulfiding process causes the Mo-OH bond to be replaced by the less acidic Mo-SH of the Mo<sup>4+</sup> ions, as suggested by Arnoldy *et al.* [20]. Also, the Figure 2 show that the acid strength of sulfides catalysts decreases with the Mo content up to 15 wt.%, then increases. The site acid of sulfides catalysts can be related with free Al-OH bonds of support together with Mo-SH bonds; therefore the decreases in the acid strength up to 15 wt.% of Mo can be attributed to decreases of free Al-OH bond of support by increases homogeneous distribution of MoS<sub>2</sub>. However, the formation of aggregates of MoS<sub>2</sub> and/or oxysulfides species over 15 wt.% of Mo could favor the slightly increases in the acid strength.

The XP spectra of all sulfided catalysts in the Mo 3d region (not shown) exhibited two partially overlapped doublets, each one containing the Mo 3d<sub>5/2</sub> and 3d<sub>3/2</sub> peaks: the binding energies (BE) of these peaks are summarized in Table 2. The primary Mo 3d<sub>5/2</sub> component of the most intense doublet remained constant (at about 229.2 eV) over the whole considered Mo loading range, corresponding closely to the value reported for Mo (V) species attributed to MoS<sub>2</sub> phase [21, 22, 23]. The Mo 3d<sub>3/2</sub> peak of the less intense doublet remains constant at BE close to 232.2 eV, and can be assigned to molybdenum oxysulfide species [24, 25]. These observations show that Mo sulfidation was incomplete due to strong interaction between the support and the Mo specie; these results are in agreement with the relative proportion of Mo (shown in parenthesis in Table 2) derived from XPS measurements. The relative proportion of surface MoS<sub>2</sub> species was around of 82 % for the catalysts with Mo loading between 10 to 17 wt.%. On the other hand, Table 2 shows that Mo/Al atomic ratio increases with the Mo loading; this behavior is better illustrated in Figure 3. The Mo/Al atomic ratio increases linearly with metal loading up to 15 wt.%; at higher Mo loadings above 15 % positive deviation from linearity was observed. This deviation over 15 % of Mo/Al atomic ratio suggests a re-dispersion of Mo species over the surface. However, EM results showed that over 15 % of Mo, occurs the formation of MoS<sub>2</sub> aggregates. Therefore, the deviation in the Mo/Al atomic ratio over 15 % must be to an overestimated experimental observed at higher Mo loadings attributed to the aggregates formation of oxysulfide

species over monolayer, leading to a lower quantity of exposed support surface and consequently an increase considerably in the Mo/Al atomic ratio. This overestimation also has been observed in the Re(x)/C catalysts by Lagos *et al.* [26].

**Table 2.** XPS binding energies (eV) and surface atomic ratios of sulfide catalysts.

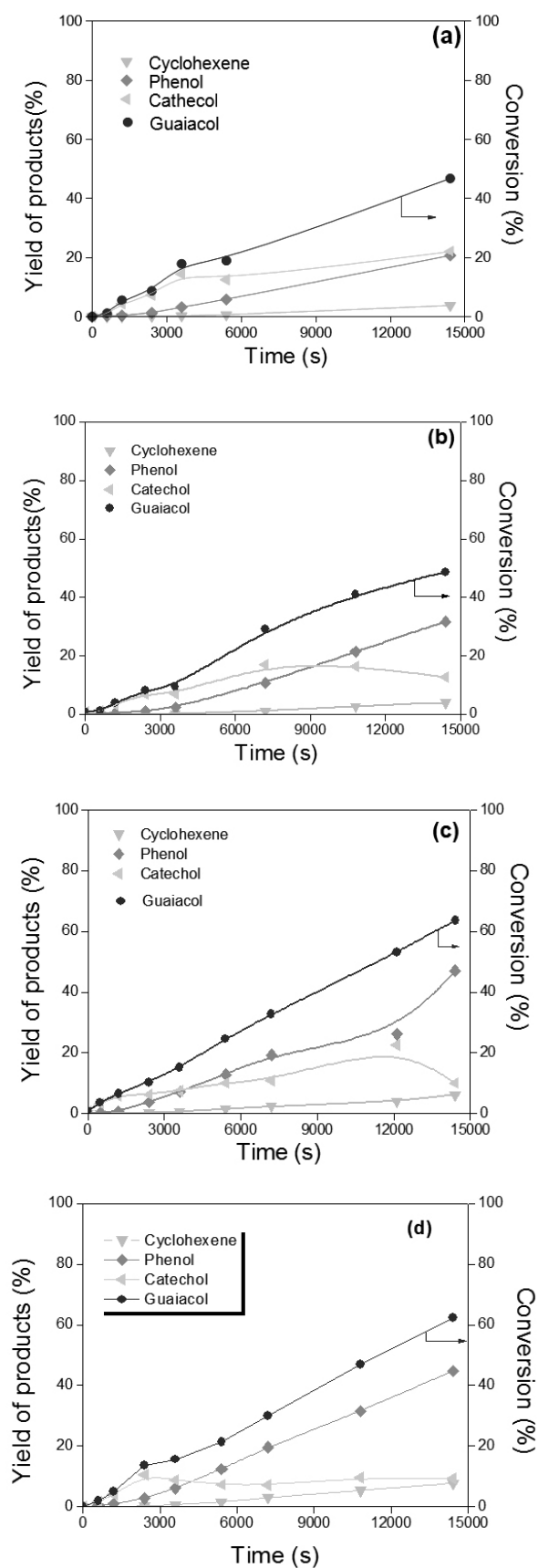
Catalysts	Al2p (eV)	Mo 3d <sub>5/2</sub> (eV)	S 2p (eV)	Mo/Al
Mo(10)/ $\gamma$ -Al <sub>2</sub> O <sub>3</sub>	74.5	229.1 (83) 232.3 (17)	162.0	0.064
Mo(12)/ $\gamma$ -Al <sub>2</sub> O <sub>3</sub>	74.5	229.2 (82) 232.3 (18)	162.0	0.080
Mo(15)/ $\gamma$ -Al <sub>2</sub> O <sub>3</sub>	74.5	229.2 (82) 232.2 (18)	162.0	0.117
Mo(17)/ $\gamma$ -Al <sub>2</sub> O <sub>3</sub>	74.5	229.2 (83) 232.2 (17)	162.0	0.156
Mo(20)/ $\gamma$ -Al <sub>2</sub> O <sub>3</sub>	74.5	229.1 (76) 232.1 (24)	162.0	0.176



**Figure 3:** Relationship between the Mo/Al atomic surface ratio and the nominal surface density of Mo for Mo(x)/ $\gamma$ -Al<sub>2</sub>O<sub>3</sub> catalysts.

### 3.2 Catalytic activity

The evolution of the transformation of guaiacol and the yield of products for the Mo(x)/ $\gamma$ -Al<sub>2</sub>O<sub>3</sub> catalysts are shown in Figure 4. The variation of the reactant and products with time can be explained by reaction schemes proposed by Laurent and Delmon [8] and complemented by Bui *et al.* [13]. On the basis of this reaction scheme, the majority of the reaction proceeded through the direct demethoxylation route (DMO) to form phenol via hydrogenolysis of the aromatic carbon-oxygen bond. The second reaction pathway involved hydrogenolysis of the O-CH<sub>3</sub> bond (demethylation route, DME) on guaiacol to form catechol, which was then transformed to phenol. Subsequently, further hydrodeoxygenation leads to benzene, hexane, cyclohexene and cyclohexane. In relation to formation of secondary products, X. Zhu *et al.* [27] found that the presence of acid sites in the catalyst favour the formation of methyl phenolic compounds (methylcatechols, methylphenols, etc.), attributed to the transferred of methyl from the methoxyl groups to the aromatic ring through acid catalyzed transalkylation reactions. This transfer can only occur when the metal is in intimate contact with the acidity of the support. In addition, some investigations have shown that the interaction of phenolic compounds with sulfided catalysts and the acid sites presents in the catalysts produces the coke poisons [8, 28-30]. In fact, Popov *et al.* [31] studied the adsorption of different phenolic groups on (Co)Mo/Al<sub>2</sub>O<sub>3</sub> catalysts demonstrated that the guaiacol anchor on the alumina support as phenate-type species, and interact also with the sulfide phase poison the active sites.



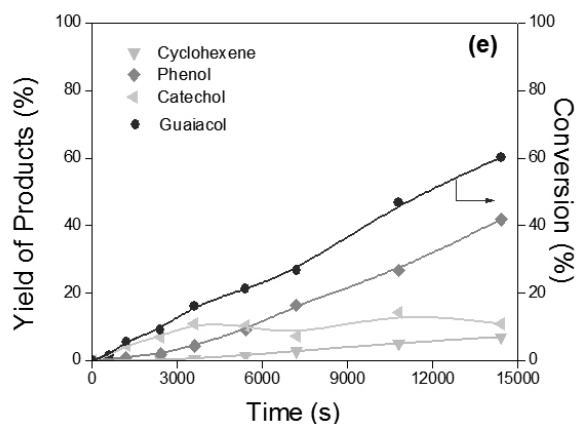


**Figure 4:** Variation of the transformation of guaiacol and the yield of products with time over Mo(x)/ $\gamma$ -Al<sub>2</sub>O<sub>3</sub> catalysts, a) 10 wt%, b) 12 wt%, c) 15 wt%, d) 17 wt% and e) 20 wt%.

**Table 3.** Catalytic activity of sulfided catalysts.

Catalysts Mo(x)/ $\gamma$ -Al <sub>2</sub> O <sub>3</sub>	Specific initial rate ( $\times 10^6 \text{ mol g}_{\text{cat}}^{-1} \text{ s}^{-1}$ )	R <sub>(phenol/catechol)</sub> (10% conv.)
Mo(10)/ $\gamma$ -Al <sub>2</sub> O <sub>3</sub>	3.04	0.21
Mo(12)/ $\gamma$ -Al <sub>2</sub> O <sub>3</sub>	3.87	0.26
Mo(15)/ $\gamma$ -Al <sub>2</sub> O <sub>3</sub>	4.28	0.55
Mo(17)/ $\gamma$ -Al <sub>2</sub> O <sub>3</sub>	3.74	0.34
Mo(20)/ $\gamma$ -Al <sub>2</sub> O <sub>3</sub>	3.22	0.34

In summary, Figure 5 shows that the principal route favoured by Mo(x)/ $\gamma$ -Al<sub>2</sub>O<sub>3</sub> catalysts for the transformation of guaiacol was the DME route. The detected products from this reaction were phenol and hydrodeoxygenated compounds, while no possible secondary products were detected.

The initial guaiacol conversion rates of all catalysts are summarized in Table 3 and illustrated in Figure 6. The initial rate increases with Mo loading up to 15 wt.% and then decreases at higher Mo loading, as demonstrated in Figure 6. The increase in the initial specific rate up to 15 wt.% loading could be attributed to an increase in the active sites due to the homogeneous distribution of Mo on the surface. Considering that the active sites in the HDO are similar to the HDS on sulfide catalysts, is possible to do the comparison in relation to morphology of sulfide catalysts. In this context, different authors proposed that hydrogenolysis/hydrogenation ratio is strongly depends of the stacking and length of sulfide catalysts [32-34]. In fact, these authors found that in the HDS reactions, the increase in the activity is correlated to the formation to the edge planes of MoS<sub>2</sub>. This is consistent with the observation that the Mo species were deposited homogeneously up to about 15 wt.% content according to the EM (in the oxide state) and XPS (in the oxysulfide state) measurements. Further increase in Mo loading leads to the formation of aggregates of oxysulfide Mo species, which are associated to decrease in the number of active sites; consequently, there is a slight decrease in initial specific rate for the conversion of guaiacol.

The selectivity, expressed by the phenol/catechol ratio calculated at 10% of conversion of guaiacol, is shown in Table 3. It can be observed that the phenol/catechol ratio increases up to 15 wt.% of Mo and then subsequently decreases. These results confirm that the phenol/catechol ratio is related with the acid strength of catalysts. In fact, the strong acid sites favour the DME route while weak acid sites favour the DMO route previously reported [11, 35].

#### 4.- CONCLUSION

The increase in the specific initial rate up to 15 wt.% of Mo loading was attributed to greater numbers of active site due to highly dispersed Mo species. Higher Mo loadings lead to the formation of Mo aggregates which causes decrease in the initial guaiacol conversion rate. On the other hand, the strong acid sites of the Mo(x)/ $\gamma$ -Al<sub>2</sub>O<sub>3</sub> sulfide catalysts favoured the DME pathway to initially produce catechol which was then converted to phenol.

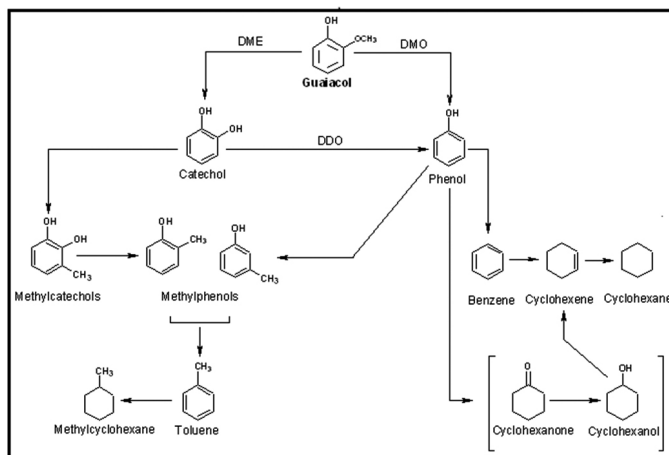


**Figure 5:** Reaction scheme of conversion of guaiacol from ref [8, 13]

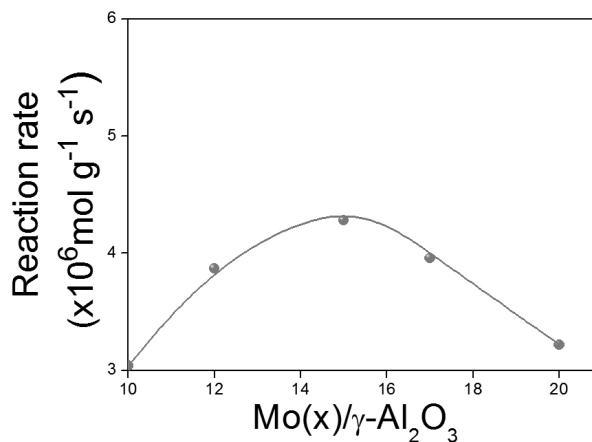


**Figure 6:** Specific initial rate of Mo(x)/ $\gamma$ -Al<sub>2</sub>O<sub>3</sub> catalysts.

#### ACKNOWLEDGMENTS

The authors thank CONICYT-Chile for FONDECYT N° 1100512, ACT-130, PFB-27 grants and Red Doctoral REDOC. CTA, MINEDUC project UCO1202 at the University of Concepción. K. Leiva is indebted to CONICYT for doctoral grant.

#### REFERENCES

- A. V. Bridgwater, S. Czernik, J. Diebold, D. Meier, A. Oasmaa, C. Peacocke, J. Piskorz, in: A. V. Bridgwater (Ed.). *Fast Pyrolysis of Biomass: A Handbook*, Antony Rowe Ltd., Chippenham, UK, (2002) 1.
- P. Grange, E. Laurent, R. Maggi, A. Centeno, B. Delmon, *Catal. Today* **29**, 297 (1996).
- V. A. Yakovlev, S. A. Khromova, O. V. Sherstyuk, V. O. Dundich, D. Yu. Ermakov, V. M. Novopashina, M. Yu. Lebedev, O. Bulavchenko, V. N. Parmon, *Catal. Today* **144**, 362 (2009).
- E. Furimsky, *Catal. Re. Sci. Eng.* **25**, 421 (1983).
- A. Gutierrez, R.K. Kaila, M.L. Honkela, R. Slioor, A.O.I. Krause, *Catal. Today* **147**, 239 (2009).
- I. T. Ghampson, C. Sepúlveda, R. Garcia, L. R. Radovic, J. L. García Fierro, N. Escalona, W. J. DeSisto, *Appl. Catal. A:Gen.* **439-440**, 111 (2012).
- P.E. Ruiz, K. Leiva, R. García, P. Reyes, J.L.G. Fierro, N. Escalona, *Appl. Catal. A:Gen* **384**, 78 (2010).
- A. Centeno, E. Laurent, B. Delmon, *J. Catal.* **154**, 288 (1995).
- J. B. Bredenberg, M. Huuska, P. Toropainen, *J.Catal.* **120**, 401 (1989).
- E. Laurent, B. Delmon, *Appl. Catal. A:Gen.* **109**, 97 (1994).

11. V. N. Bui, G. Toussaint, D. Laurenti, C. Mirodatos, C. Geantet, *Catal. Today*, **143**, 172 (2009).
12. V. Bui, D. Laurenti, P. Afanasiev, C. Geantet, *Appl. Catal. B*, **101**, 239 (2011).
13. V. Bui, D. Laurenti, P. Delichère, C. Geantet, *Appl. Catal. B*, **101**, 246 (2011).
14. E.J.M. Hensen, P.J. Kooyman, Y. van der Meer, A.M. van der Kraan, V.H.J. de Beer, J.A.R. van Veen, R.A. van Santen, *J. Catal.*, **199**, 224 (2001).
15. Y.Q. Yang, C.T. Tye, K.J. Smith, *Catal. Commun.*, **9**, 1364 (2008).
16. R. Cid, G. Pechi, *Appl. Catal.*, **14**, 15 (1985).
17. F. J. Gil-Llambías, M. Escudéy, *J. C. S. Chem. Commun.*, 478 (1982).
18. N-Y. Topsøe, H. Topsøe, *J. Catal.*, **139**, 631 (1993)
19. P. Sarrazin, S. Kastelan, E. Payen, J.P. Bonnelle, J. Grimblot, *J Phys Chem.*, **97**, 5954 (1993).
20. P. Arnoldy, J. A. M. van den Heijkant, G. D. de Bok, J. A. Moulijn, *J. Catal.*, **92**, 35 (1985).
21. A.-F. Lamic, A. Daudin, S. Brunet, C. Legens, C. Bouchy, E. Devers, *Appl. Catal. A:Gen.*, **344**, 198 (2008).
22. A. C. B. dos Santos, P. Grange, A.C. Faro Jr, *Appl. Catal. A:Gen.*, **178**, 29 (1999).
23. J. Grimblot, P. Dufresne, L. Gengembre, J.P. Bonnelle, *Bull. Soc. Chim. Belg.*, **90**, 1261 (1981).
24. J. Ramirez, R. Cuevas, A. López-Agudo, *Appl. Catal. A:Gen.*, **57**, 223 (1990).
25. B. Pawelec, R.M. Navarro, J.M. Campos-Martin, A. López Agudo, P.T. Vasudevan, J.L.G. Fierro, *Catal. Today*, **86**, 73 (2003).
26. G. Lagos, R. García a, A. López Agudo, M. Yates, J. L.G. Fierro, F.J. Gil-Llambías, N. Escalona, *Appl. Catal. A:Gen.*, **358**, 26 (2009).
27. X. Zhu, L. L. Lobban, R. G. Mallinson, D. E. Resasco, *J Catal.*, **281**, 21 (2011).
28. M. Badawi, S. Cristol, J.-F. Paul, E. Payen, *C. R. Chim.*, **12**, 754 (2009)
29. M. Badawi, J.-F. Paul, S. Cristol, E. Payen, *Catal. Commun.*, **12**, 901 (2011).
30. E. Laurent, A. Centeno, B. Delmon, *Stud. Surf. Sci. Catal.*, **88**, 573 (1994).
31. A. Popov, E. Kondratieva, L. Mariey, J. M. Goupil, J. E. Fallah, J.-P. S. Silvasanker, A.V. Ramaswamy, P. Ratnasamy In: Barry MF, Mitchell PCH (eds), Proc 3rd Int Conf on Chemistry and Uses of Molybdenum, Climax Molybdenum Company, 1979; p 98.
32. S. J. Tauster, T. A. Pecoraro, R. R. Chianelli, *J. Catal.*, **63**, 515 (1980).
33. H. Topsøe, R. Candia, N-Y Topsøe, B. Clausen, *Bull Soc Chim Belg.*, **93**, 783 (1984).
34. K. Leiva, C. Sepúlveda, R. García, J. L. G. Fierro, G. Águila, P. Baeza, M. Villarroel, N. Escalona, *Appl. Catal. A: Gen.*, **467**, 568 (2013).